Available online at www.sciencedirect.com
ScienceDirect
Sensors and Actuators B 128 (2008) 388–398
SENSORS AND ACTUATORS B CHEMICAL
www.elsevier.com/locate/snb

Measurement of pH and dissolved oxygen within cell culture media using a hydrogel microarray sensor

Seungjoon Lee [a], Bennett L. Ibey [a], Gerard L. Coté [a,*], Michael V. Pishko [b]

[a] *Department of Biomedical Engineering, Texas A&M University, College Station, TX 77843, United States*
[b] *Departments of Chemical Engineering, Chemistry, and Materials Science & Engineering The Pennsylvania State University, University Park, PA 16802, United States*

Received 24 March 2007; received in revised form 16 June 2007; accepted 25 June 2007
Available online 30 June 2007

Abstract

The sensing of analytes in cell culture media without the introduction of exogenous reagents proves difficult in today's cell culturing systems. In this paper, a completely embeddable microarray sensor that has been developed along with a compact fluorescent imaging system to sense oxygen and pH non-invasively is described. The compact detection system consists of an ultra-bright blue diode source, coupling optics, interference filters and a compact moisture resistant CCD camera. The microarray sensor was created by photoreaction injection molding and contains two separate sensing elements. The system was constructed and the array tested using simple spiked buffer solutions and complex cell media. In addition, the system was coupled to a bioreactor and tested over 2 weeks. The standard error of prediction during a bioprocess for both oxygen and pH detection was 0.75% and 0.092, respectively. The time response of the sensor in the designed flow-through arrangement was less than 90 s for both pH and oxygen, well within that needed for cell culture monitoring. Overall, this sensing approach has promise as a lab-on-a-chip type sensor for complete sensing of the culture environment and eventually may be used in a feedback system that allows monitoring and control without human intervention.

Keywords: Poly(ethylene glycol); Fluorescent sensing; Cell culture

1. Introduction

Well-controlled cell culture experiments are paramount to the conduct of biomedical and scientific research. Current cell culturing is performed in a sterile environment optimized for laboratory-based experiments.[1–3] Standard protocols for cell culture and the analytical monitoring of the media require repeated exposure of cells to the natural (non-sterile) environment at times where media is refreshed and different agents are added. This process is typically well controlled and, with the help of antibacterial and antifungal agents, results in low incidence of contamination. This process, however, is very time consuming and requires a high amount of human interaction to be successful [1–3]. A fully automated system that can maintain both cell viability and control of media composition would benefit research areas employing cell culture. Towards this goal, a sensing system capable of detecting the parameters most influential to cell health (pH, oxygen, glucose, and lactate), that monitors in a non-invasive and non-interactive manner requiring little human intervention, needs to be developed [4]. The design, construction and testing of such a sensing system for pH and oxygen is the topic of this article.

Electrochemical sensing has proven repeatable and dependable over time for its use in laboratories [5]. Silver chloride pH meters are laboratory instruments which require external calibration and maintenance. The Clark electrode for measuring oxygen similarly requires calibration and maintenance, but is dependable and repeatable with proper calibration. These methods of sensing oxygen and pH are proven, but do not allow for unperturbed monitoring over time in a sterile culture environment because of the need for a portal into the system and direct interaction with the cell media. Optical sensors are innately non-invasive and, if completely enclosed into the culturing system, could allow for a non-invasive system that requires minimal maintenance after initial installation/calibration. The sensing

* Corresponding author. Tel.: +979 862 1076; fax: +979 845 4450.
E-mail addresses: sjlee@tamu.edu (S. Lee), bli6339@tamu.edu (B.L. Ibey), gcote@tamu.edu (G.L. Coté), mpishko@engr.psu.edu (M.V. Pishko).

0925-4005/$ – see front matter © 2007 Elsevier B.V. All rights reserved.
doi:10.1016/j.snb.2007.06.027

device includes a microarray sensor placed within an optical window connecting directly to the cell culturing system. This path allows media to flow unhindered across the sensing element and return to the cell culturing system, thus conserving media. A custom optical system, which is both inexpensive and portable, has been developed to image the sensing array and relay that information to a processing unit. This system could ultimately be connected to chambers containing various chemicals and automatically exchange or fortify the cell media in response to the measured chemical changes. The development of such a system not only has importance to earth-based laboratory settings, but is valuable to experiments based in Space where limited human involvement is desired. This system is easily transferable into a cell bioreactor based system for that purpose.

The dominant feature of the sensing system is the fluorescent hydrogel array, which interacts directly with the cell culture media. Preliminary work was performed by this group for the development of a poly(ethylene glycol) (PEG) hydrogel oxygen sensor based on the quenching reaction between oxygen and a ruthenium organometallic complex [4]. In this work, it was shown that a sensor slab (1 cm × 1 cm) could sense changes in dissolved oxygen between 0 and 21% at a rate effectively equal to that of the standard Clark electrode. The physical sensor used in this research was a thin film sensor measuring 1 cm × 1 cm with a thickness of approximately 180 μm. Another previous work on lithographically securing hydrogel sensing elements to silicon and silica surfaces has proven effective through surface modification with 3-(trichlorosilyl) propyl methacrylate (TPM) [6]. In this previous paper, single arrays (single sensing chemistry) were constructed and tested by repeated exposure of the target chemical under a fluorescence microscope. The response and stability over time proved to be within the parameters for implementation into a cell culturing system. Here the aim was the development of both a combined multianalyte sensor on a single chip and a low cost optical detection system to image the sensor array. The array developed in this paper included both an oxygen-sensitive ruthenium organometallic complex for oxygen detection and a pH sensitive fluorescent dye for the detection of pH changes. More specifically, dichlorotris (1,10-phenanthroline) ruthenium(II) hydrate (Ru(Phen)) and 2′,7′-bis-(2-carboxyethyl)-5-(and-6)-carboxyfluorescein–dextran conjugate (BCECF) were the two fluorescent compounds which have been chosen for use in this sensing array to detect changes in oxygen and pH, respectively. Fluorescent transition metal complexes containing ruthenium have been studied for use in oxygen sensors because oxygen quenches their fluorescent emission [7]. This quenching can be probed through 488 nm excitation (absorption peak) and collection of emission light above 500 nm (peak fluorescence 610 nm). Ruthenium complexes are known to have high quantum efficiency, high photostability, and large Stoke's shift, making them an optimum choice for a microarray sensor. The quenching reaction, which takes place when ruthenium interacts with oxygen, is described by the Stern–Volmer quenching equation. This relation suggests a linear relationship between the percent loss in fluorescence and the concentration of dissolved oxygen [8]. The use of fluorescent sensors to measure pH has also been widely studied [9,10]. Most fluorophores show an innate sensitivity to pH, which appears as either intensity changes or a wavelength shift in the emission or absorption spectrum. For both agents, direct intensity measurement is most simple but may not be accurate because of photobleaching and light source variation that are not distinguishable from intensity change due to the concentration change of analyte. To overcome this problem, ratiometric measurement, fluorescence lifetime, or using internal standard were employed over the years [11–15]. These techniques, however, require a complicated/expensive system (such as cooled CCD, time resolving electronics, or additional dichroic filters/mirrors), and are thus not suitable for a compact portable system which is essential for bioreactor applications. In addition, unwanted intensity variations can be minimized or eliminated by reducing photobleaching and using stable source/detector. Due to the need for simplicity in the devised sensing system, a fluorophore whose intensity changes with pH was chosen rather than ratiometric pH sensitive agents. Fluorescein isothiocyanate labeled dextran (FITC-dextran) was our first choice, but proved to photobleach far too quickly to produce reliable signal over time. To remedy this, a modified fluorescein based compound (BCECF-dextran) was chosen due to its greater photostability over FITC-dextran [9,16]. The spectral characteristics of both agents and filters are shown in Fig. 1.

Implementing these fluorescent probes into a microarray requires an encapsulation material that allows for unhindered diffusion of the target analyte, but restricts leaching of the sensing chemistry. Previous sensing approaches have entrapped sensing agents into various materials including sol–gels, silicone, polymers, and silica gels [17–29]. These encapsulation materials work well, however, for optimum biocompatibility and increased diffusion of the target analytes, PEG was employed by our group. PEG hydrogels permit rapid diffusion of the target molecule, while having a mesh size small enough to entrap the sensing chemistry. This polymer also has improved biocompatibility and is resistant to bio-fouling and degradation within biological environments [30,31]. In a recent publication, the effectiveness of sensing oxygen fluorescently by entrapping ruthenium complexes in a permeable PEG hydrogel sensor has

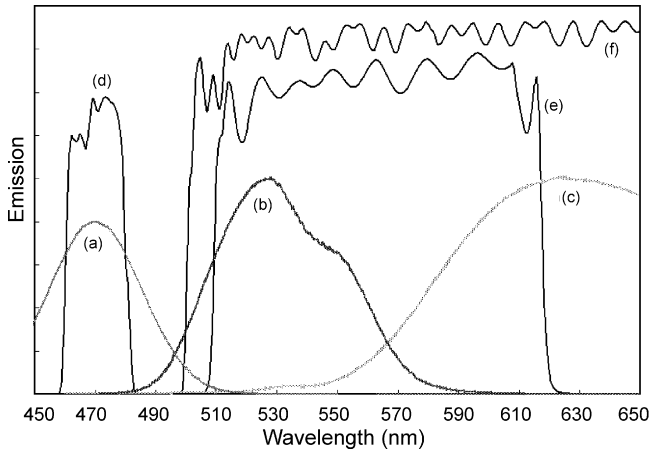

Fig. 1. Emission spectra of LED (a), BCECF-dextran (b), ruthenium complex (c), and transmittance spectra of optical filters (d–f).

been shown [32]. In subsequent publications, the use of PEG to encapsulate fluorescent pH, nitric oxide, glucose, and oxygen sensors in individual PEG was shown [4,6,33,34]. This article describes the combination of previous single element sensing arrays into a single multi-element microarray sensor for measurement of oxygen and pH simultaneously. This combination is complicated by the need to develop an optical system capable of sensing both signals independently through a closed flow system, which is also described. The functionality of the optical system and microarray sensor is tested in spiked buffer solutions and verified using cell culture media.

2. Experimental

2.1. Chemicals and materials

Liquid poly(ethylene glycol) diacrylate (PEG-DA) with an average molecular weight of 575, 3-(trichlorosilyl) propyl methacrylate (TPM), 6N sulfuric acid, *n*-heptane, dichlorotris (1,10-phenanthroline) ruthenium(II) hydrate, Cytodex® microcarrier beads, and Dulbecco's modified Eagle's medium (DMEM) without phenol red were purchased from Sigma–Aldrich (St. Louis, MO). Trypsin-EDTA, penicillin-streptomycin, and bovine calf serum was purchase from Gibco (Carlsbad, CA). 2′,7′-Bis-(2-carboxyethyl)-5-(and-6)-carboxyfluorescein–dextran conjugate (BCECF-dextran, 70,000 MW) was purchased from Molecular probes (D-1880, Carlsbad, California). 2-Hydroxy-2-methyl-1-phenyl-1-propanone (Darocur® 1173) was obtained from Ciba Specialty Chemicals (Tarrytown, NY). Deionized water with a resistance of 18 MΩ cm was used for all aqueous experiments (Millipore, Billerica, MA). Poly(dimethyl siloxane) (PDMS) elastomer was purchased from Dow Corning Sylgard 184 (Midland, MI), which is composed of a prepolymer and curing agent. The chrome sodalime photomask was purchased from Advanced Reproductions (Andover, MA). SU-8 50 negative photoresist and developer was purchased from Microlithography Chemical Corp (Newton, MA). All other chemicals were commercially available and used without further purification.

2.2. Fabrication of microfluidic device

Autocad® was used to devise a pattern of 6 parallel microchannels 100 μm wide and 100 μm apart. This design was then patterned to a chrome-quartz photomask by Advanced Reproductions. SU-8 50 was spin-coated (2000 rpm) onto a silicon wafer and the wafer was cured through the photomask using long-wavelength UV to create a pattern on the silicon wafer with 50 μm height. A PDMS mold containing microchannels (inverse of the pattern on the silicon wafer) was created by curing a 10:1 mixture of PDMS prepolymer and curing agent against the SU-8 50 patterned silicon. This mold was cured for a 24 h at 60 °C, removed, and extensively washed with water and 75% alcohol. Holes were punched at each side of the microchannels using a 16-gauge needle to create inlet ports. A detailed fabrication method is presented elsewhere [35,36].

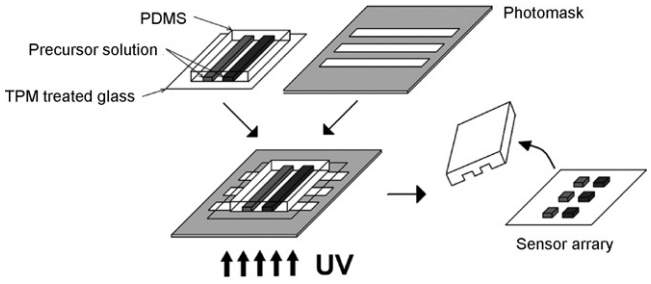

Fig. 2. Depicted is a schematic of the photolithography procedure used to create the microarray sensors. Precursor solution was injected into PDMS channels on the surface modified glass. After UV exposure through a photomask, sensor array was obtained.

2.3. Hydrogel sensor fabrication

The hydrogel-based pH and oxygen sensors were constructed using a modified procedure to bind PEG hydrogels to glass substrate. In short, the hydrogel arrays were patterned photolithographically with PEG-DA on glass substrates as depicted in Fig. 2 [35]. To prepare the substrates for the hydrogel microstructures, an oxidized surface was created by using a sulfuric acid wash for at least 4 h, followed by a sodium hydroxide 1 M wash for at least 4 h. The oxidized glass was treated with 3-(trichlorosilyl)propyl methacrylate (TPM) in a hexane and carbon tetrachloride mixture (3:1) to form a self assembled monolayer (SAM) with pendant methacrylate groups. Two different precursor solutions were prepared for each analyte. For the pH sensitive elements, the precursor solution was made by mixing PEG-DA (60%, v/v), photo-initiator (2%, v/v), BCECF-dextran solution at 1 mg/mL concentration (10%, v/v), and water (28%, v/v). For the oxygen sensitive elements, the precursor solution was made by mixing PEG-DA (60%, v/v), photo-initiator (2%, v/v), ruthenium complex solution at 5 mg/mL concentration (2%, v/v), and water (36%, v/v). The concentration of each fluorophore was determined to have similar fluorescent dynamic range under experimental conditions. The volume ratio of PEG-DA and photoinitiator was kept constant to ensure identical hydrogel structure for each sensor element. Both precursor solutions were mixed with a vortex mixer. The PDMS made using the above procedure was affixed to the treated glass slide and allowed to dehydrate for 24 h to seal the microchannels. Precursor solution was injected into each microchannel and cured by UV light (EFOS Ultracure 100SS Plus) that was projected through the chrome photomask for 2 s (300 mW/cm^2, λ_{peak} = 365 nm) to form the hydrogel arrays. After curing, the PDMS replica was removed from the glass slide and the slide was washed to remove uncured solution. The final sensor contained two arrays with three elements in each, allowing for measurement of two independent chemicals in triplicate. The excess glass surrounding the array was removed by cleaving to reduce the size of the final sensor.

2.4. Optical imaging system

An optical detection system was developed to capture the fluorescence image of the sensor array. As depicted in Fig. 3, a

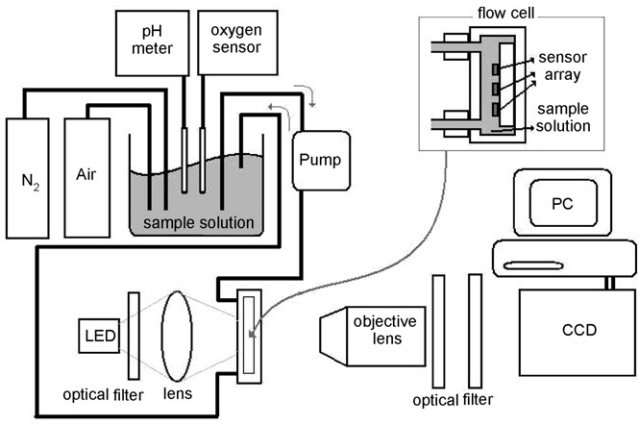

Fig. 3. Depicted is a schematic of the custom optical setup that images the sensor array through the flow-through optical window. This setup consists of a blue diode light source which is collimated by optics and projected onto the sample. The fluorescent light is separated from the excitation light by filtering and the camera captures the fluorescent image. The inset picture displays a zoomed-in version of the flow cell.

blue LED with a 7° half intensity beam angle ($\lambda_{peak} = 470$ nm, $\lambda_{FWHM} = 40$ nm, Opto Diode Corp., CA) served as the illumination source for the sensor array. An optical bandpass filter ($\lambda_{center} = 470$ nm, $\lambda_{FWHM} = 20$ nm, Chroma Technology Corp, VT) was used as an excitation filter and a lens ($f = 50$ mm) served to focus the light onto the sensor. A gas-impermeable quarts flow cell (face detachable) with 2 mm pathlength (Starna Cells. CA) was used as the sample chamber and sensor holder. The sensor was placed inside the flow cell and sample solutions were pumped over the sensor by a peristaltic pump. A microscope objective lens (10×) was used to focus the fluorescence image onto a monochrome CCD camera (Hitachi Denshi America, NY). A 500 nm cut-off longpass filter and a bandpass filter ($\lambda_{center} = 560$ nm, $\lambda_{FWHM} = 100$ nm) were used to remove excitation light. The CCD camera was controlled by a PC and all captured images were stored for data analysis. The voltage supply to the LED was set to 3.0 V–90 mA (max power at 3.7 V–300 mA) to minimize photobleaching. The exposure time for all images was 2 s.

2.5. Characterization of sensor with buffer

As depicted in Fig. 3, phosphate buffered saline solution (PBS, 0.1 M) was placed into a beaker and a pH meter (Thermo, Waltham, MA) and a standard Clark electrode oxygen sensor (MI-730, Microelectrodes, Bedford, NH) were used to externally monitor pH and O_2. The commercial oxygen sensor was calibrated at the start of experiment using two water standards; nitrogen gas (0% O_2) and air (21% O_2). The commercial pH meter was calibrated with standard buffer solutions. To build the pH calibration model, pH was changed across a range of pH 5.8 to 8.2 by adding acid/base in the solution while the dissolved oxygen level was kept at 21% with continuous bubbling of air. The fluorescence image was captured and readings from the pH and oxygen electrode sensors were recorded. This step was repeated at 0% dissolved oxygen level. To build the oxygen calibration model, the oxygen level was changed from 0 to 21% by bubbling and air/N_2 mixture into the solution while the pH was kept constant at pH 6.0. The fluorescence images were captured and readings from the pH and oxygen electrode sensors were recorded. This step was repeated at pH 7.0 and 8.0, respectively. For validation, a table was made to have 20 spiked pH (6.0–8.0) and dissolved oxygen (3–21%) values with zero correlation. The pH and dissolved oxygen level of the solution was adjusted to follow the spiked sample table. Data was collected similarly for each pH and oxygen level.

2.6. Characterization of the sensor with cell culture media

The buffer solution was replaced by Dulbecco's modified Eagle's medium (DMEM) without phenol red supplemented with 4 mM L-glutamine, 1.5 g/L sodium bicarbonate, antibiotics, and bovine calf serum (10%, v/v), which is a common formula for mammalian cell culture. Calibration and prediction data for the DMEM were collected in the same manner as described in the previous section.

2.7. Characterization of sensor with cell culture media during a bioprocess

Cell culture media was prepared with Dulbecco's modified Eagle's medium (DMEM) without phenol red supplemented with 4 mM L-glutamine, 1.5 g/L sodium bicarbonate, 4.5 g/L glucose, 200 U/mL penicillin, 200 μg/mL streptomycin and bovine calf serum 10% (v/v). Fibroblast cells (NIH/3T3) were purchased from ATCC (Manassas, VA). The initial pH of the cell culture media was 7.4 and the cells were grown in a polystyrene tissue culture flask to the desired quantity for the experiment. During the cell culture, the temperature and CO_2 levels were kept constant at 37 °C and 5% by an incubator (NuAire, Plymouth, MN). When the cells were grown to the desired quantity, some of the cells were inoculated into the bioreactor and the others were frozen at −80 °C with complete growth medium supplemented with dimethyl sulfoxide (DMSO, 10%, v/v).

The Synthecon (Houston, TX) Rotary Cell Culture System (RCCS) was used for cell culturing. The system has core filter inside of the vessel to prevent cell leakage. The entire system was sterilized before addition of cell culture media and cell inoculation. All of the components to be autoclaved, including a quartz flow cell which is used as the sensor holder, were filled with 75% ethyl alcohol for 24 h and then rinsed with deionized water and cleaned before autoclaving. The components were disassembled, wrapped with aluminum foil, and placed inside of the autoclave. After autoclaving, all of the components were exposed to UV light for 24 h in a laminar flow bench to ensure sterile conditions. The entire system was reassembled in a laminar flow bench in reverse order of the disassembly. After autoclaving and reassembly, the RCCS was filled with the cell culture media. When the rotating wall vessel was almost full, microcarriers (autoclaved in a 0.1 M PBS solution prior to use) and cells were inoculated through injection ports on the side of the rotating wall vessel. Initial cell concentration was 3.1×10^5 cells/mL and microcarrier concentration was 3 g/L (dry weight). After coupling to the flow cell with the microar-

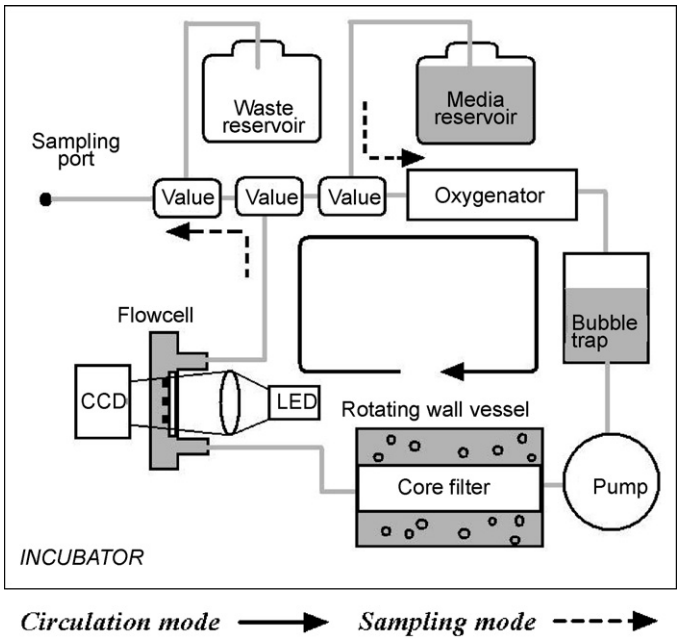

Fig. 4. A diagram of optical setup coupled with a bioreactor. Media sampling was performed five times per day for 2 weeks. Media is circulating through the vessel, pump, flowcell, and oxygenator during circulation mode while fresh media goes into the reactor and old media is collected through a sampling port during sampling mode.

ray sensor, the reactor and imaging system were placed in an incubator.

Calibration data were acquired off-line before cell inoculation using the same manner as described in the previous section. The temperature of solution was kept at 37 °C so as to have the same condition as the bioprocess. A schematic diagram for the cell culture experiment is shown in Fig. 4. The rotating wall vessel and the core filter were kept rotating at 10 rpm as recommended by the manufacturer. The pumping speed of the peristaltic pump was adjusted to have 2 mL/min flow rate as recommended by the manufacturer. The cell culture media was circulated through the rotating wall vessel, flow cell, valves, bubble trap, and oxygenator by the pump. The fluorescence image of the sensor was captured using the previously developed imaging system in the same manner as the calibration step. For the sample collection, three-way valves were manipulated for injection of fresh cell culture media and ejection of old cell culture media. The reactor sampling port, commercial pH probe, and commercial oxygen probe were placed in a 15 mL centrifuge tube to measure actual pH and O_2. The tube was filled with cell culture media up to 10 mL and each probe reading was recorded. Those two procedures were performed five times per day over 2 weeks as follows: right before media refreshing (media refreshing was performed every 24 h by injecting 200 mL of fresh media to increase pH to over 7.0), 1 h after media refreshing, 3 h after media refreshing, 6 h after media refreshing, and 12 h after media refreshing. Oxygenation of the RCCS is normally maintained at a constant dissolved oxygen level in the cell culture media. Thus, it was expected that the sensor response to oxygen would be a flat line over the experimental period. In order to test the sensor with greater dynamic range, oxygenation was intentionally stopped for 3 h (between 3 h after media refreshing and 6 h after media refreshing) every day. This was performed by stopping the peristaltic pump and oxygenator fan. The standard error of calibration (SEC) and the standard error of prediction (SEP) were calculated in the same manner as described in the previous section.

2.8. Sensor response time and stability

Sensor response time was measured by continuous data collection during a rapid concentration change of each analyte. The experimental setup was identical to the off-line experimental setup. Sensor stability was tested by using a single sensor over each experiment. Photostability was tested with continuous exposure to the light source. Between each experiment, the sensor was stored in a buffer solution under light tight conditions at room temperature. The sensor was sterilized with 75% alcohol prior to each experiment.

2.9. Image processing

All fluorescence images were analyzed with MATLAB 6.5® (Natick, MA). Each image was cropped to contain six elements (three elements of each sensor type) resulting in an image size of 50 × 70 pixels (total 3500 pixels). The average intensity value within each element was calculated to have three intensity values for pH and three for oxygen. Based on calibration data for pH and dissolved oxygen, a calibration curve was obtained by applying either linear or polynomial curve fitting. Predicted pH and dissolved oxygen was calculated by applying the intensity value from the spiked sample of the calibration curve and compared to the readings from the commercial pH and oxygen electrode sensors.

3. Results and discussion

3.1. Hydrogel sensor fabrication

The main goal of this work was to build a microarray sensor sensitive to various analytes of interest. This chip-like sensor has an advantage in bioprocess monitoring over optical fiber based sensors because the fabrication is based on replicate PDMS molding, which yields microstructures of high reproducibility. The process is simple, inexpensive, and easy to perform in a sterile manner, and lastly, the optical system measures both the signal of interest and the sensor itself which enables monitoring of the sensor. Moreover, once the sensor is placed inside of a cell culture system, contamination can be avoided since it is isolated from the outside environment. To verify reproducibility, several sensor chips were fabricated with the same PDMS mold and the fluorescence intensity image of each sensor was compared under the same environmental conditions (pH, O_2, and source intensity). The images gave the same fluorescence intensity for each sensor chip (0.1% standard deviation), verifying reproducibility and batch-to-batch consistency in the fabrication process.

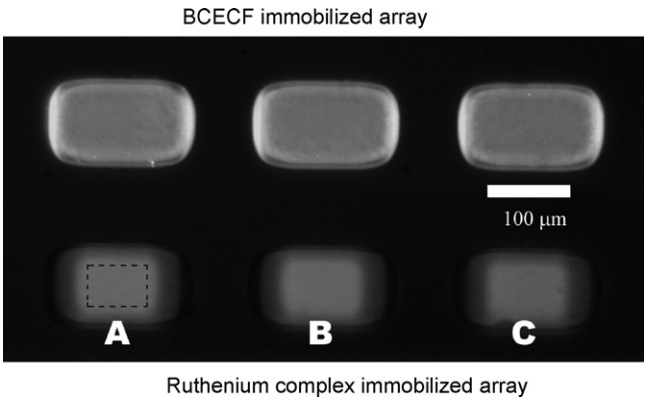

Fig. 5. Depicted is an image of the sensor as captured by the camera. The top row contains BCECF and the bottom row contains the ruthenium complex. It can be seen that signal loss on the edges of the ruthenium sensors is evident due to swelling and leaching and therefore box A is used as the average fluorescent signal.

3.2. Image processing

An example of the sensor image is shown in Fig. 5. The ruthenium complex immobilized array (bottom three) shows that there was initial leaching of dye around the edges which is not observed in BCECF-dextran immobilized array (top three). It is well known that hydrogels swell in the presence of water [37,38]. It was shown that the hydrogel structure swells unevenly since the bottom of the structure is bound to the glass surface while the top is free to swell [36]. This inhomogeneous swelling causes a looser mesh density on the top and the side of the sensor, resulting in leaching of fluorophores. The leaching of ruthenium is critical for biological applications because of its potential toxicity. No additional leaching, however, was observed after the initial swelling. This was confirmed because the same intensity level was observed before and after experiments. The BCECF-dextran immobilized array did not leach because of the large molecular structure of the complex. The change in signal from the initial leaching around the edges was removed by processing the data based on the center area of the array which proved to be uniform for both sensor arrays (dashed line in Fig. 5). This rectangular area at the center of each array (50 × 70 pixels) was cropped, averaged, and used for data analysis. As depicted in Fig. 6(a), the averaged pixel value of areas A–C (in Fig. 5) at different oxygen levels were slightly different because of the excitation beam non-uniformity. The excitation beam from the diode source was collimated using a microscope objective to a nearly homogenous beam, however, slight variations in intensity over the beam profile translated into a difference in the baseline luminescence between individual elements of the sensor array. After background subtraction, depicted in Fig. 6(b), the normalized intensity shows consistent response to oxygen level. For the data shown, only the center element of each sensor was required for image analysis.

3.3. Characterization of sensor with buffer

To evaluate the sensor's sensitivity to each analyte of interest, the sensor was tested in buffer solutions with various pH/O_2 levels as described above. For the pH sensor calibration, pH was gradually increased and decreased at a constant dissolved oxygen level and repeated for different constant dissolved oxygen levels. For the oxygen sensor calibration, dissolved oxygen was increased and decreased at a constant pH and was repeated at different constant pH values. Fig. 7 shows the sensor response to pH (a) and dissolved oxygen (b) from the calibration data. Both sensors show sensitivity, repeatability and reversibility. Correlation (less than 0.1) ensures that crosstalk between sensors is not considerable. One major concern in fluorescence-based sensing is the potential for photobleaching which is a permanent or semi-permanent destruction of the luminescent properties of the fluorescent probe. The fluorescent emission of BCECF-dextran was stable under LED exposure (∼5 min total exposure time). Within the tested pH range (pH 5.8–8.2). Fig. 8 shows

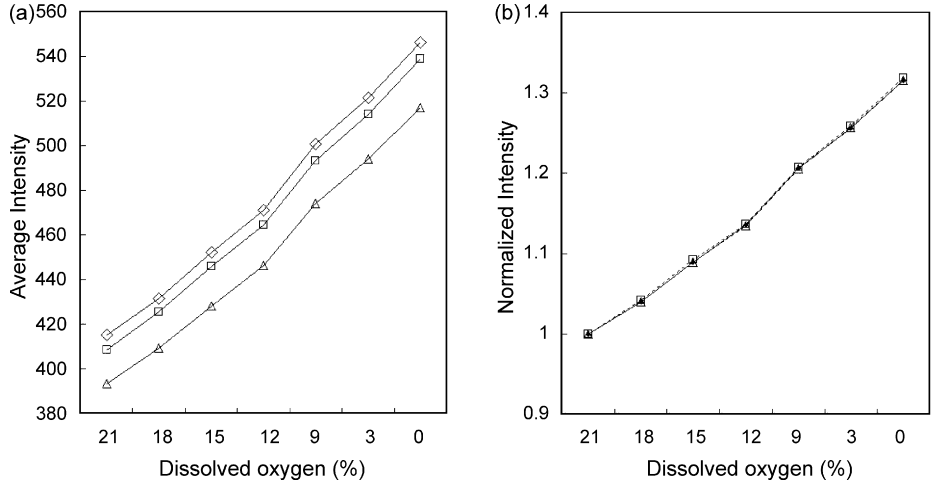

Fig. 6. In this figure the sensor response of the three individual oxygen sensing elements from 0 to 21% dissolved oxygen level is depicted. The raw intensity data (a) shows that there are baseline differences between the sensing elements due to the non-uniform light source, but the response to changing oxygen is the same. The normalized data (b) shows that the individual response curves of the three sensing elements are identical and therefore the inhomogeneous excitation beam does not affect the oxygen measurement.

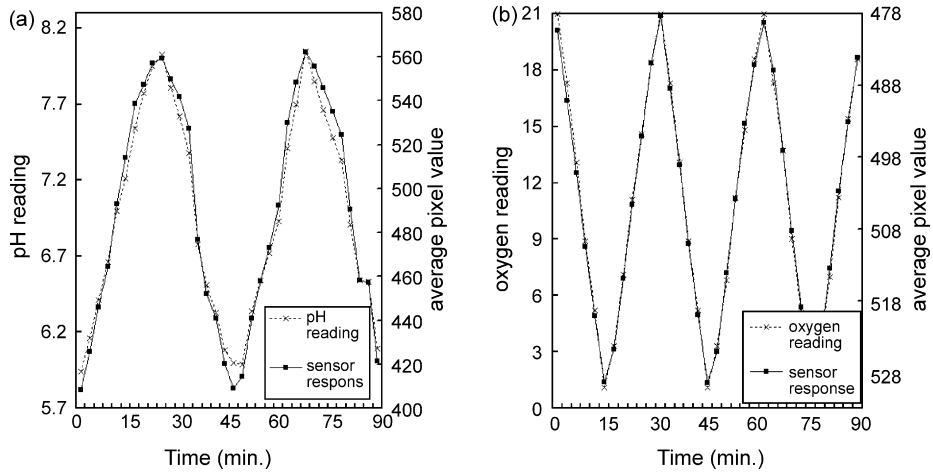

Fig. 7. The response (a) of the BCECF sensing element to a controlled pH titration during a calibration is displayed. This process was performed twice, showing the reversibility of the sensor. The actual pH was verified using a commercial pH probe. The response (b) of the ruthenium sensing element to a ramped oxygen titration is displayed. This process was performed three times, showing the reversibility of the sensor. The actual dissolved oxygen concentration was verified using a commercial Clark electrode.

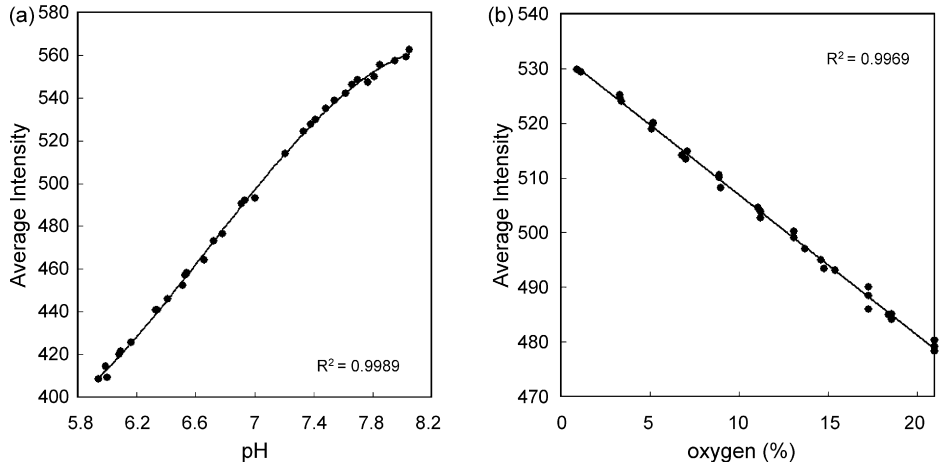

Fig. 8. The calibration data used to generate the curve for the pH is shown in (a) in which the commercial probe was used to determine pH. The data was acquired randomly and the data fits a sigmoidal model well. The calibration data used to generate the curve for the oxygen is shown in (b) using the commercial Clark Electrode to determine percent oxygen. The data was acquired randomly and the data fits the linear Stern–Volmer model well.

the calibration data for pH (a) and oxygen (b), respectively. The pH sensor shows a sigmoidal response to pH which is nearly identical to free BCECF-dextran in solution [39]. A third order polynomial fitting was applied to build the pH calibration curve because it was easy to trace the sigmoidal response. Within the tested pH range, third order polynomial fitting successfully traced the pH sensor response ($R = 0.9989$). Linear regression was applied to build the oxygen calibration model which agrees with the Stern–Volmer quenching model at low concentration ($R = 0.9969$). Table 1 shows the prediction results of pH and oxygen based on the fluorescence image intensity of the spiked sample. The intensity was applied to the calibration model and pH/O_2 was predicted and compared to the commercial electrode sensor reading. The standard error of prediction (SEP) was 0.07 units for pH and 0.64% for oxygen. The error sources include the response time of the sensor and/or delays in the flow system between the water bath and sensor array and differences between local pH/oxygen in the sensor and in the sample chamber because the spiked sample testing required rapid changes of pH or oxygen.

Table 1
The standard error of calibration (SEC) and standard error of prediction (SEP) for pH and dissolve oxygen in buffer and cell culture media

	Buffer (PBS)		Cell media (DMEM) off-line		Cell media (DMEM) on-line	
	pH	Oxygen (%)	pH	Oxygen (%)	pH	Oxygen (%)
SEC	0.068	0.62	0.071	0.62	0.063	0.59
SEP	0.070	0.64	0.072	0.65	0.092	0.75

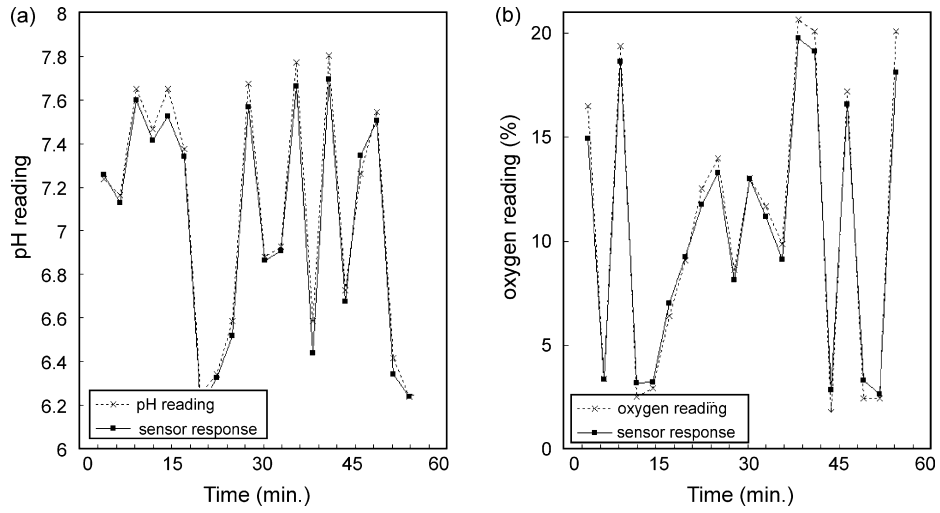

Fig. 9. The response of hydrogel sensor and commercial probes to the spiked pH (a) and oxygen (b) during a validation run is displayed. The prediction data was acquired by randomly changing the pH and the dissolved oxygen concurrently in a cell culture media sample. The plot shows good agreement between our sensor and the commercial sensor.

3.4. Characterization of sensor with cell culture media

The sensor was tested in cell culture media off-line to verify that the sensor can be used for bioprocess monitoring. Calibration/prediction was performed in the same manner as previously described for the buffer solutions. Calibration data were similar to buffer case and not shown here. As shown in Fig. 9, the sensor responded to the spiked pH (a) and dissolved oxygen (b). The plot of predicted pH and dissolved oxygen versus commercial probe reading (Fig. 10) from the spiked sample shows that the sensor response reliably monitored pH and dissolved oxygen in cell culture media. As shown in Table 1, the SEP was 0.07 units for pH and 0.65% for oxygen which is nearly identical to the results with buffer. These results show that the sensor was able to monitor pH and dissolved oxygen in a more complex media such as cell culture media.

3.5. Characterization of sensor with cell culture media during a bioprocess

In order to test the feasibility of the microarray sensor for use in bioprocess monitoring, the sensor and imaging system was coupled to a bioreactor and tested over 2 weeks. The sensor image was collected five times per day and analyte concentration was predicted based on the calibration model that was acquired in the off-line calibration. Fig. 11(a) shows a plot of fluorescent probe predicted and commercial probe measured pH. The result clearly shows that the sensor response is reliable for monitoring pH in the cell culture media. In a 24 h period, the pH of media decreased as nutrients were taken up by the cells and as the levels of respiratory by-products (mostly acidic) increased. The pH of the media returned back to the optimal range when the media was refreshed every 24 h. Fig. 11(b) shows a plot of pH measured by the commercial sensor versus pH predicted

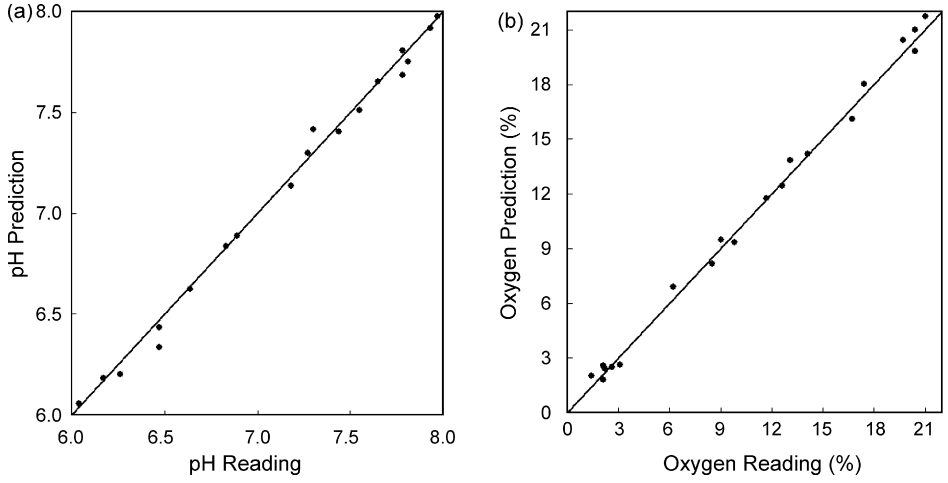

Fig. 10. The plot of predicted value vs. commercial probe reading for pH (a) and dissolved oxygen (b) from spiked cell culture media is displayed. The plot shows good agreement between our sensor and the commercial sensor over the tested range of pH and dissolved oxygen, respectively.

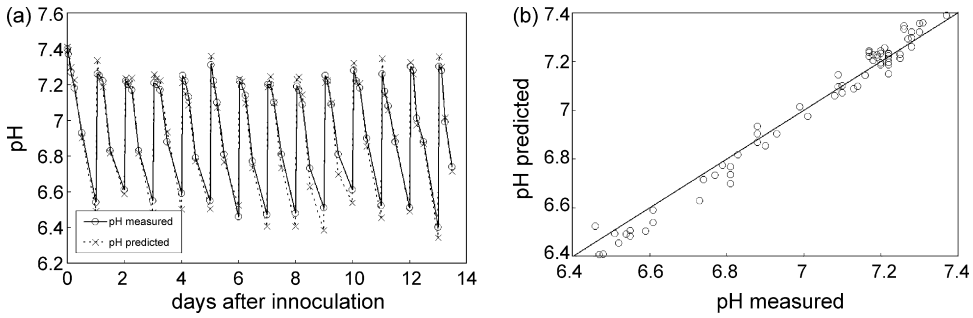

Fig. 11. pH sensor response during a bioprocess. Plot (a) shows good agreement between the microarray pH sensor and the commercial sensor for 2 weeks. In addition, plot (b) shows minimal bias or drift.

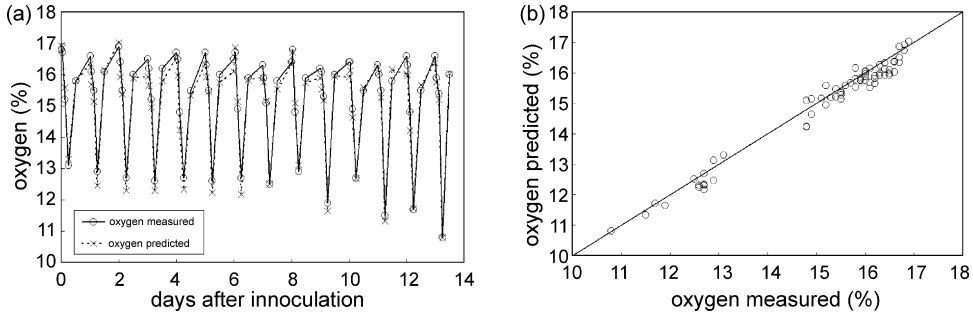

Fig. 12. Oxygen sensor response during a bioprocess. Plot (a) shows good agreement between microarray oxygen sensor and the commercial sensor for 2 weeks. In addition, plot (b) shows minimal bias or drift.

by the microarray sensor. The result shows that the sensor was able to monitor pH of cell culture media on-line for 2 weeks with minimal bias or drift. Fig. 12(a) shows a plot of O_2 prediction and O_2 measured by a commercial probe sensor. The result shows that the sensor response is reliable for monitoring dissolved oxygen in the cell culture media. For the cell proliferation, oxygen in cell culture media is consumed by respiratory activity of the cells. An oxygenator was used in this bioreactor to maintain oxygen level as well as carbon dioxide level. However, the oxygenation was stopped for 3 h per day to verify the sensor's dynamic range. As shown in Fig. 12(a), the O_2 level dropped below 13% when the oxygenator was stopped, and the sensor was able to sense the change in dissolved oxygen level. The O_2 level of the media went back up to the optimal range after re-running the oxygenator. Fig. 12(b) shows a plot of O_2 measured by a commercial sensor versus O_2 predicted by the microarray sensor. The results show that the sensor was able to monitor the dissolved oxygen level of cell culture media on-line for 2 weeks. The prediction error for pH and O_2 was 0.09 and 0.75%, respectively (Table 1). The overall errors increased slightly compared to the off-line experiments and were likely due in part to system variation, sensor degradation, or photo/chemical bleaching. The accuracy of the microarray was not better than the commercial electrode sensors (typically 0.01 unit for pH and 0.1% for oxygen), but had the added advantages of being small and totally enclosed in the system, for noninvasive monitoring with no contamination, unlike the commercial probes that are indwelling and thus tethered to the external electronics.

3.6. Sensor response time and stability

The sensor response time was tested by inducing a rapid change in the concentration of each analyte. As shown in Fig. 13, 90% of the sensor's response was achieved in 48 s for a change in pH from 6.0 to 8.0 and 24 s for a change in dissolved oxygen from 21 to 0%. After 90 s, both sensors responded to each target analyte at maximum dynamic range. The migration of a proton or oxygen molecule into the hydrogel structure is dom-

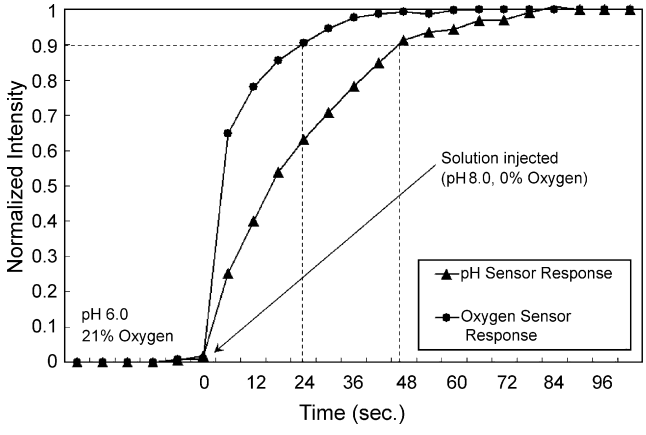

Fig. 13. The time response of the sensor from the minimum to maximum within the range of interest (0–21% oxygen and 6–8 pH) is shown. This response curve shows that the sensor response for the pH sensor is slower than that of the dissolved oxygen and that after about 50 s both have fully reacted to the change in analyte concentration. This time response is adequate for use of this sensor in a cell culturing system where concentrations are not expected to change rapidly.

inated by natural diffusion and presumed to be the reason for the slow response time. Therefore, this response time can be reduced by decreasing the size of each array to maximize the surface area to volume ratio. Alternatively increasing the mesh size of the structure by using a decreased volume ratio of PEG-DA in the precursor solution would also speed up this diffusion, but may induce further leaching. However, the current response time is adequate for use in bioprocess monitoring since it does not require the measurement of rapid analyte concentration changes.

After each experiment, the sensor was stored in buffer (PBS 0.01 M, pH 7.0) without exposure to ambient light. The sensors used for the above experiments did not exhibit any noticeable dye leaching, or physical degradation over 2 weeks. Since each exposure time was 2 s, total exposure time of each sensor was not over 5 min. Under 5 min of continuous exposure to the current light source, less than 1% intensity drop was observed for both agents. The sensors were also sterilized with 75% ethanol and no loss in function was observed after multiple sterilizations. This data confirms that the sensor's lifetime is useful for a typical cell culture experiment and that the sensors can be sterilized, proving their potential for non-invasive monitoring.

4. Conclusions

This work has described the development of a multi-analyte sensitive hydrogel microarray sensor constructed via microfluidic patterning of hydrogel structures to monitor pH and dissolved oxygen concentration simultaneously in cell culture media. It also described the development of an optical imaging system to quantify the analyte concentration based on fluorescence intensity of the sensor. Highly cross-linked PEG hydrogels were fabricated using UV induced photopolymerization of acrylated PEGs. These hydrogels were hydrophobic, optically transparent, and easily manipulated. In addition, they were able to be anchored to glass slides and easily encapsulated functional agents for use as biosensors. BCECF-dextran and ruthenium complex were used as the sensing agents and immobilized into the hydrogel structures. A series of tests for sensitivity, stability, reversibility, and temporal/spatial uniformity were performed and revealed the feasibility for use in bioreactor applications. The sensor was viable after sterilization with ethanol, proving it can be used in bioprocess monitoring without introducing contamination. A compact and inexpensive optical system was developed to capture the fluorescence image of the hydrogel microarray sensor with a LED, a series of optical filters and lenses, a quartz flow cell and a monochrome CCD camera. All of the components were commercially available and inexpensive compared to complicated microscopic imaging systems. The imaging system was sufficiently reliable for this application and its compact size enabled operation inside of a typical incubator. The sensor and the imaging system was combined and introduced into a bioreactor for monitoring media during 2 weeks of fibroblast cultivation. It was established that the sensor was capable of measuring pH and dissolved oxygen during a typical bioprocess in cell culture media across the biological range required for mammalian cell culture. The hydrogel-based sensor was non-intrusive after placement inside the bioprocess system, was constructed using a simple and highly reproducible manufacturing method, and had a response time adequate for cell culture monitoring. The results presented in this study suggest that this technique can be extended to introduce more sensing agents, allowing for a complete lab-on-a-chip technology for cell culture monitoring. Further research would include making microarrays with sensing agents capable of detecting glucose, lactate, and nitric oxide. In addition to the introduction of more sensing agents, further miniaturization of the sensor chip and optical system would allow for an inexpensive modulated portable monitoring system capable of disposable sensor implementation for cell culturing systems.

Acknowledgments

The authors acknowledge the support of the National Aeronautics and Space Administration (Grant BIOTECH 01-0023-0131). BLI acknowledges the support of a Graduate Assistance in Areas of National Need (GAANN) Fellowship.

References

[1] L. Ksinantova, J. Koska, R. Kvetnansky, M. Marko, D. Hamar, M. Vigas, Effect of simulated microgravity on endocrine response to insulin-induced hypoglycemia in physically fit men, Horm. Metab. Res. 34 (2002) 155–159.
[2] S.A. Rosario, G.S. Cha, M.E. Meyerhoff, M. Trojanowicz, Use of ionomer membranes to enhance the selectivity of electrode-based biosensors in flow-injection analysis, Anal. Chem. 62 (1990) 2418–2424.
[3] T. Yao, Y. Nanjyo, H. Nishino, Micro-flow in vivo analysis of L-glutamate with an on-line enzyme amplifier based on substrate recycling, Anal. Sci. 17 (2001) 703–708.
[4] D.P. O'Neal, M.A. Meledeo, J.R. Davis, B.L. Ibey, V.A. Gant, M.V. Pishko, G.L. Coté, Oxygen sensor based on the fluorescence quenching of a ruthenium complex immobilized in a biocompatible poly(ethylene glycol) hydrogel, IEEE Sens. J. 4 (2004) 728–734.
[5] J.M. Zen, A.S. Kumar, D.M. Tsai, Recent updates of chemically modified electrodes in analytical chemistry, Electroanalysis 15 (2003) 1073–1087.
[6] J. Zguris, M.V. Pishko, pH sensitive fluorescent poly(ethylene) glycol hydrogel microstructures for monitoring in cell culture systems, Sens. Lett. 3 (2005) 206–210.
[7] J.N. Demas, D. Diemente, E.W. Harris, oxygen quenching of charge-transfer excited-states of ruthenium(II) complexes—evidence for singlet oxygen production, J. Am. Chem. Soc. 95 (1973) 6864–6865.
[8] J.R. Lakowicz, Principles of Fluorescence Spectroscopy, 2nd ed., Kluwer Academic/Plenum Press, New York, 1999.
[9] P. Richard, Handbook of Fluorescent Probes and Research Products, 9th ed., Molecular Probes, 2002.
[10] L.L. Song, E.J. Hennink, I.T. Young, H.J. Tanke, Photobleaching kinetics of fluorescein in quantitative fluorescence microscopy, Biophys. J. 68 (1995) 2588–2600.
[11] C.G. Niu, X.Q. Gui, G.M. Zeng, A.L. Guan, P.F. Gao, P.Z. Qin, Fluorescence ratiometric pH sensor prepared from covalently immobilized porphyrin and benzothioxanthene, Anal. Bioanal. Chem. 383 (2005) 349–357.
[12] S.B. Bambot, G. Rao, M. Romauld, G.M. Carter, J. Sipior, E. Terpetchnig, J.R. Lakowicz, Sensing oxygen through skin using a red diode-laser and fluorescence lifetimes, Biosens. Bioelectron. 10 (1995) 643–652.
[13] H. Szmacinski, J.R. Lakowicz, Optical measurements of ph using fluorescence lifetimes and phase-modulation fluorometry, Anal. Chem. 65 (1993) 1668–1674.
[14] H. Szmacinski, J.R. Lakowicz, Fluorescence lifetime-based sensing and imaging, Sens. Actuat. B: Chem. 29 (1995) 16–24.
[15] H.A. Clark, R. Kopelman, R. Tjalkens, M.A. Philbert, Optical nanosensors for chemical analysis inside single living cells. 2. Sensors for pH and cal-

cium and the intracellular application of PEBBLE sensors, Anal. Chem. 71 (1999) 4837–4843.
[16] I.D. Weiner, L.L. Hamm, Use of fluorescent dye bcecf to measure intracellular ph in cortical collecting tubule, Am. J. Physiol. 256 (1989) F957–F964.
[17] O.S. Wolfbeis, M.J. Leiner, H.E. Posch, A new sensing material for optical oxygen measurement, with the indicator embedded in an aqueous phase, Mikrochim. Acta 3 (1986) 359–366.
[18] I. Klimant, O.S. Wolfbeis, Oxygen-sensitive luminescent materials based on silicone-soluble ruthenium diimine complexes, Anal. Chem. 67 (1995) 3160–3166.
[19] X.M. Li, F.C. Ruan, K.Y. Wong, Optical characteristics of a ruthenium(II) complex immobilized in a silicone-rubber film for oxygen measurement, Analyst 118 (1993) 289–292.
[20] J.F. Gouin, F. Baros, D. Birot, J.C. Andre, A fibre-optic oxygen sensor for oceanography, Sens. Actuat. B: Chem. 39 (1997) 401–406.
[21] M.F. Choi, D. Xiao, Single standard calibration for an optical oxygen sensor based on luminescence quenching of a ruthenium complex, Anal. Chim. Acta 403 (2000) 57–65.
[22] T. Miyashita, J.F. Chen, M. Yuasa, M. Mitsuishi, Fabrication of polymer organized thin films containing ruthenium complexes, Polym. J. 31 (1999) 1121–1126.
[23] C. Preininger, I. Klimant, O.S. Wolfbeis, Optical-fiber sensor for biological oxygen-demand, Anal. Chem. 66 (1994) 1841–1846.
[24] K.P. McNamara, X.P. Li, A.D. Stull, Z. Rosenzweig, Fiber-optic oxygen sensor based on the fluorescence quenching of tris(5-acrylamido, 1,10-phenanthroline) ruthenium chloride, Anal. Chim. Acta 361 (1998) 73–83.
[25] E. Singer, G.L. Duveneck, M. Ehrat, H.M. Widmer, Fiber optic sensor for oxygen determination in liquids, Sens. Actuat. A: Phys. 42 (1994) 542–546.
[26] W. Wang, C.E. Reimers, S.C. Wainright, M. Shahriari, M.J. Morris, Applying fiber-optic sensors for monitoring dissolved oxygen, Sea Technol. 40 (1999) 69–74.
[27] C. Malins, M. Niggemann, B.D. MacCraith, Multi-analyte optical chemical sensor employing a plastic substrate, Meas. Sci. Technol. 11 (2000) 1105–1110.
[28] C.M. Ingersoll, F.V. Bright, Using sol gel-based platforms for chemical sensors, Chemtech 27 (1997) 26–31.
[29] B.D. Maccraith, G. Okeeffe, C. Mcdonagh, A.K. Mcevoy, LED-based fiber optic oxygen sensor using sol–gel coating, Electron. Lett. 30 (1994) 888–889.
[30] K.L. Prime, G.M. Whitesides, Self-assembled organic monolayers—model systems for studying adsorption of proteins at surfaces, Science 252 (1991) 1164–1167.
[31] J.L. West, J.A. Hubbell, Photopolymerized hydrogel materials for drug-delivery applications, React. Polym. 25 (1995) 139–147.
[32] R.J. Russell, M.V. Pishko, A.L. Simonian, J.R. Wild, Poly(ethylene glycol) hydrogel-encapsulated fluorophore-enzyme conjugates for direct detection of organophosphorus neurotoxins, Anal. Chem. 71 (1999) 4909–4912.
[33] J. Zguris, M.V. Pishko, Nitric oxide sensitive fluorescent poly(ethylene glycol) hydrogel microstructures, Sens. Actuat. B: Chem. 115 (2006) 503–509.
[34] R.M. Rounds, B.L. Ibey, H.T. Beier, M.V. Pishko, G.L. Coté, Microporated PEG spheres for fluorescent analyte detection, J. Fluoresc. 17 (2007) 57–63.
[35] W.G. Koh, M. Pishko, Photoreaction injection molding of biomaterial microstructures, Langmuir 19 (2003) 10310–10316.
[36] A. Revzin, R.J. Russell, V.K. Yadavalli, W.G. Koh, C. Deister, D.D. Hile, M.B. Mellott, M.V. Pishko, Fabrication of poly(ethylene glycol) hydrogel microstructures using photolithography, Langmuir 17 (2001) 5440–5447.
[37] P.J. Flory, J. Rehner, Statistical mechanics of cross-linked polymer networks. II. Swelling, J. Chem. Phys. 11 (1943) 521–526.
[38] M.B. Mellott, K. Searcy, M.V. Pishko, Release of protein from highly cross-linked hydrogels of poly(ethylene glycol) diacrylate fabricated by UV polymerization, Biomaterials 22 (2001) 929–941.
[39] D.A. Russell, R.H. Pottier, D.P. Valenzeno, In-vivo spectroscopic properties of the fluorescent ph indicator biscarboxyethyl carboxyfluorescein, J. Photochem. Photobiol. B 29 (1995) 17–22.

Biographies

Seungjoon Lee received the B.S. degree in mechanical engineering from Yonsei University, Seoul, Korea, in 2000 and the M.S. and Ph.D. degrees in biomedical engineering from Texas A&M University in 2003 and 2006, respectively. Currently, he is a postdoctoral researcher within the Department of Biomedical Engineering at Texas A&M University. His research interests are in the development of optical analyte monitoring systems for biological applications, signal and image processing, and optical simulations.

Bennett L. Ibey received the B.S. degree in biomedical engineering from Texas A&M University (TAMU), College Station, in 2001 and his Ph.D degree in biomedical optics at the Optical Bio-sensing Laboratory, TAMU, in 2006. His research topics included fluorescence based analyte detection and blood-perfusion sensing by pulse oximetry. Dr. Ibey is a member of the Biomedical Engineering Honor Society, Alpha Eta Mu Beta, the Delta Chapter of Tau Beta Pi, Phi Kappa Phi Honor Society, Golden Key Honor Society, and National Society of Collegiate Scholars. He was a recipient of the Graduate Assistance in Areas of National Need Fellowship and was awarded the Whitaker International Postdoctoral Fellowship.

Gerard L. Coté is Head of the Department of Biomedical Engineering and holds the Charles H. and Bettye Barclay Professorship in Engineering at Texas A&M University. He joined the Texas A&M Engineering faculty in 1991 as an assistant professor and was named professor in 2002. Dr. Coté directs the Optical Biosensing Laboratory, where research focuses on the development of macro-scale to nano-scale systems using lasers, fiberoptics and electronics for new, noninvasive ways to test blood sugar levels in diabetes; to detect other body chemicals such as beta amyloid for Alzheimer's disease; to detect analytes in cell culture; and to diagnose cancer. Dr. Coté has had funded research from NIH, NSF, NASA, private foundations, and private companies resulting in over 180 journal publications, proceedings, and presentations. He has written three book chapters and is a co-holder of four U.S. patents. He is a co-founder of two small medical device companies BioTex, Inc. and Visualase Inc. He is a Fellow of the American Institute for Medical and Biological Engineering. Dr. Coté received his master's and Ph.D. in bioengineering from the University of Connecticut, Storrs in 1987 and 1990 respectively. He received a bachelor's degree in electrical engineering from the Rochester Institute of Technology in 1986.

Michael Pishko is the Unocal Professor and Head of the Department of Chemical Engineering, Texas A&M University. Prior to joining the faculty at Texas A&M, he held the rank of Distinguished Professor at Penn State University from 2001 to 2007. He received his B.S. and M.S. in chemical engineering from the University of Missouri-Columbia and his Ph.D. in chemical engineering from the University of Texas at Austin. He also received postdoctoral training at the Massachusetts Institute of Technology. The Pishko group investigates the synthesis, microfabrication, and clinical application of biosensors and biomaterials. For his research, he has received an NSF CAREER award, was named an Alfred P. Sloan Research Fellow, and was elected to the College of Fellows, American Institute for Medical and Biological Engineering. He currently serves as an Associate Editor for the IEEE Sensors Journal. Dr. Pishko has co-authored over 90 peer-reviewed publications and is a co-inventor of 19 issued U.S. patents.